RSC Advances

PAPER

View Article Online
View Journal | View Issue

Check for updates

Cite this: *RSC Adv.*, 2022, **12**, 17005

Low temperature magnetic behavior and thermal expansion anomaly of cubic $CeTiO_3$

Jiandi Li,[a] Aijun Gong, *[ab] Lina Qiu,[a] Xin Yang,[a] Zongren Zhang,[a] Weixiong Feng,[a] Yuzhen Bai,[a] Yiwen Wang[a] and Rongrong Fan[c]

Received 20th February 2022
Accepted 22nd April 2022

DOI: 10.1039/d2ra01137a

rsc.li/rsc-advances

Lanthanum-based $LnBO_3$ perovskite oxides have demonstrated fascinating magnetic properties and spin–lattice coupling. In this work, we report an unusual thermal expansion anomaly coupled with the magnetic ordering in the cubic $CeTiO_3$ with the vacancy of Ce ions. The magnetic behaviors and lattice thermal expansion at low temperature were systematically investigated using the temperature dependence of the magnetization measurements and low temperature X-ray powder diffraction. It is clearly revealed that there are two magnetic transitions in the cubic $CeTiO_3$ from 5 to 350 K: one is a magnetic ordering–disordering transition at 300 K and the other one might be a change of the magnetic component near 32 K. Both the magnetization and hysteresis change correspondingly upon cooling. Intriguingly, a lattice thermal expansion anomaly is found below the magnetic ordering temperature, which indicates a strong coupling of spin and lattice, *i.e.*, a magnetovolume effect (MVE). Our findings provide the possibility of adjusting thermal expansion behavior and magnetic properties by introducing a vacancy of Ln atoms in lanthanum-based perovskite oxides.

Introduction

Lanthanum $LnBO_3$-based perovskite oxides have demonstrated fascinating performances in ionic conductivity,[1] photoelectricity,[2] catalysis,[3] ferroelectric and magnetism.[4,5] By adjusting the chemical composition appropriately, the crystal structure together with charge and electronic structure can be facilely manipulated, which triggers the lattice distortions of BO_6-octahedra and engineers the unusual physical properties.[6,7] For instance, giant magnetoresistance effects emerge in $Ln_{1-x}Ca_xMnO_3$,[8,9] $Ln_{1-x}Sr_xMnO_3$ (ref. 10) and $Ln_{1-x}Ba_xMnO_3$ solid solutions.[11] Although the origin of the magnetoresistance has remained controversial to date, the superexchange interaction, *i.e.*, transformation from Mn^{3+} to Mn^{4+}, will emerge in Mn^{3+}–O^{2-}–Mn^{4+} linkage under a magnetic ordering state.[12,13] The itinerant electron is sensitive to the applied magnetic field and the resistance can be tuned accordingly in these materials.[14,15]

The magnetism of $LnTiO_3$ perovskite oxides is always restricted to low temperature, generally less than 200 K. Ideal $CeTiO_3$ shows an orthorhombic symmetry (space group: *Pnma*). The oxygen non-stoichiometry (*i.e.* deficiency and excess) can bring about the change of the charges of Ce and Ti, which may induce intriguing physical properties. In our previous work, an unconventional cubic $CeTiO_3$ sample (space group: $Fd\bar{3}m$) was synthesized by sol–gel method (Fig. 1).[16] The cation Ce

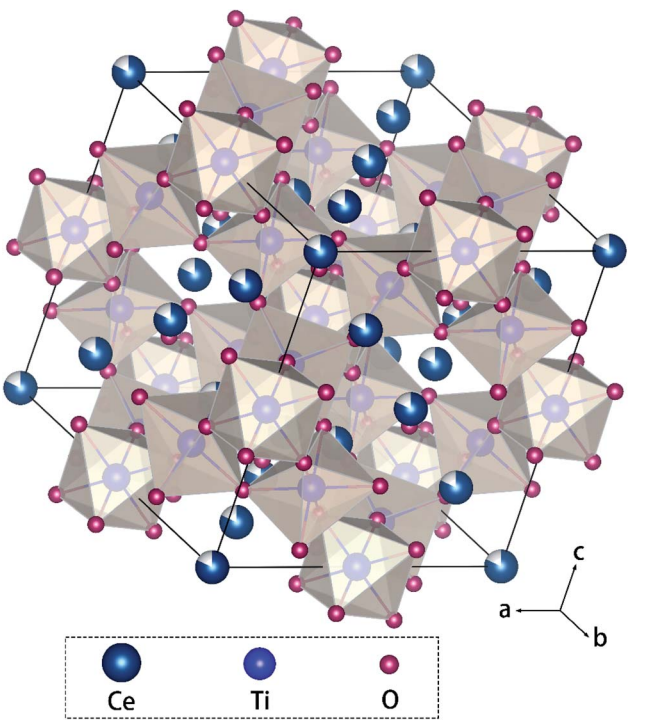

Fig. 1 Crystal structure of cubic $CeTiO_3$ compound with the vacancy of Ce ions.

[a]College of Chemistry and Biological Engineering, University of Science and Technology Beijing, Beijing 100083, China. E-mail: gongaijun5661@ustb.edu.cn
[b]Beijing Key Laboratory for Science and Application of Functional Molecular and Crystalline Materials, University of Science and Technology Beijing, Beijing 100083, China
[c]Kunshan Hexin Mass Spectrometry Technology Co, Ltd, Jiangsu, 215300, China

Open Access Article. Published on 07 June 2022. Downloaded on 4/27/2026 4:14:30 AM.
This article is licensed under a Creative Commons Attribution-NonCommercial 3.0 Unported Licence.

Open Access Article. Published on 07 June 2022. Downloaded on 4/27/2026 4:14:30 AM.
This article is licensed under a Creative Commons Attribution-NonCommercial 3.0 Unported Licence.

coordinates with 12 O anions and Ti coordinates with 6 anions. The structure shows obvious vacancy of Ce ions and is stable with temperature. The unusual weak magnetic state persists up to 400 K, which is very rare for Ce–Ti–O perovskites.[17,18] The magnetic behavior might be different at low temperature, but remains poor knowledge. This inspires us to investigate the magnetic behavior with respective to temperature.

Here, we carry out temperature dependence of magnetization measurements and low temperature X-ray powder diffraction to systematically study the magnetic behaviors and lattice thermal expansion at low temperature. It is clearly revealed that magnetic ordering emerges upon cooling down to 300 K and the hysteresis become larger as the magnetic component changes. Intriguingly, lattice thermal expansion anomaly is found below magnetic ordering temperature, which indicates a strong coupling of spin and lattice, *i.e.*, magneto-volume effect (MVE). This work gives a good example of

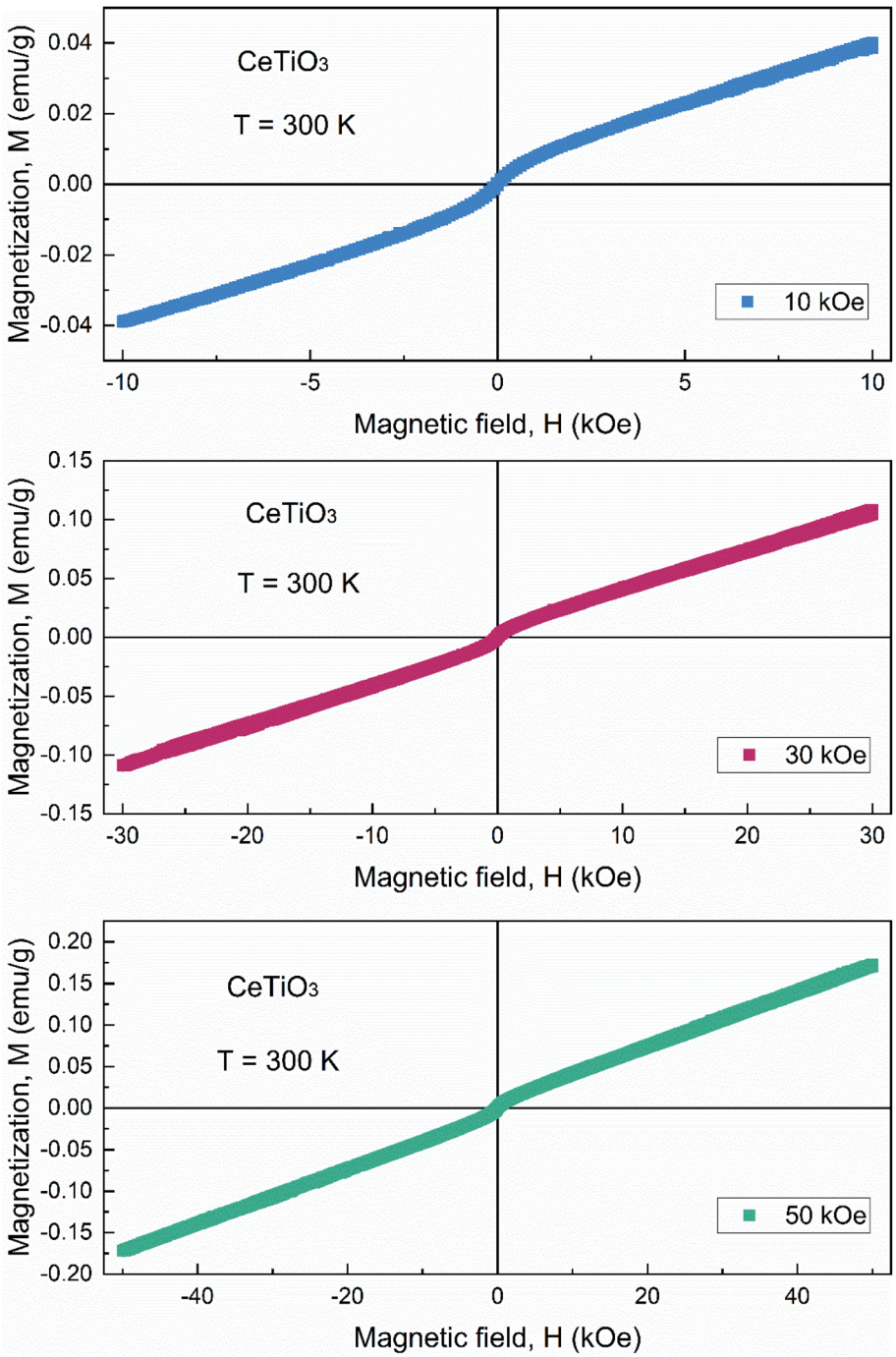

Fig. 2 Magnetization *vs.* applied magnetic field (*M*–*H*) curve of $CeTiO_3$ measured at 300 K with variable maximum of magnetic fields.

© 2022 The Author(s). Published by the Royal Society of Chemistry

Open Access Article. Published on 07 June 2022. Downloaded on 4/27/2026 4:14:30 AM.
This article is licensed under a Creative Commons Attribution-NonCommercial 3.0 Unported Licence.

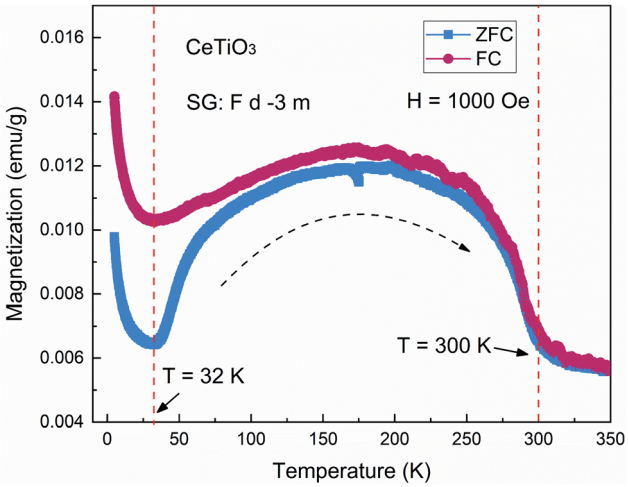

Fig. 3 Temperature dependence of magnetization curves for $CerTiO_3$ under zero field cooling and field cooling (ZFC–FC) with constant field of 1000 Oe from 5 to 350 K. The arrows indicate there might be magnetic transition at that temperature.

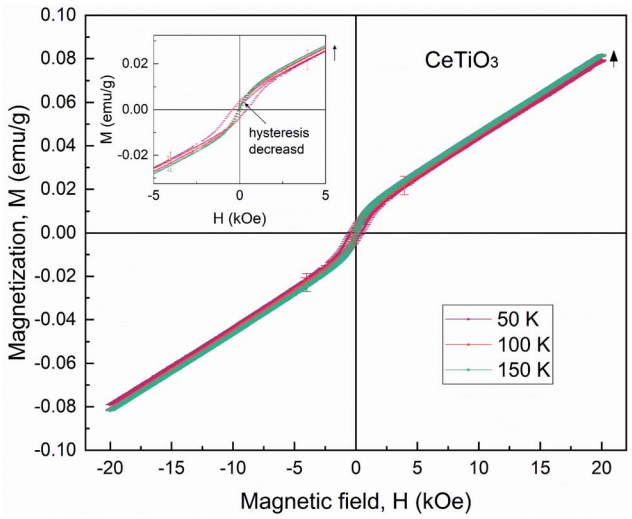

Fig. 5 Magnetization *vs.* applied magnetic field (*M*–*H*) curve of $CeTiO_3$ measured at 50 K, 100 K and 150 K, respectively.

exploring unusual magnetic behaviors in $LnBO_3$-based perovskite oxides.

Experimental

Cerium oxide, $CeTiO_3$, was prepared by using sol–gel methods.[19,20] The details are as follows: The 10 mL water was added by mixing 6.8 mL of tetrabutyl titanate and 10 mL of glacial acetic acid, and added to the above solution under strong stirring to obtain a clear Ti precursor solution. Ti precursor solution was taken, rare earth nitrate solution of 1.64 g was added to the corresponding stoichiometry, and 4 mol L^{-1} citric acid aqueous solution of 3 mL was finally added. As the evaporation continues with stirring, the solution gradually precipitates and becomes a gel subsequently. The gel was dried at 120 °C for 12 h, to obtain a foam-loose porous dry gel. After grinding, the powder was placed in the rover furnace for 2 h at 200 °C to remove the organic crosslinking, then raised to 400 °C in an air atmosphere and maintained for 2 h, and then 800 °C for 4 h, cooling with the furnace, grinding to be used.

The magnetization *vs.* applied magnetic field (*M*–*H*) curves were measured using physical property measurement system (PPMS) (Quantum Design, Inc., USA) from 5 to 400 K. The maximum magnetic field was from −50 to 50 kOe. The magnetization *vs.* temperature (*M*–*T*) curves were measured under zero field cooling and field cooling (ZFC–FC) with $H =$ 1000 Oe from 5 to 350 K. The warming rate was 5 °C min^{-1}. Temperature dependence of XRD data were measured on

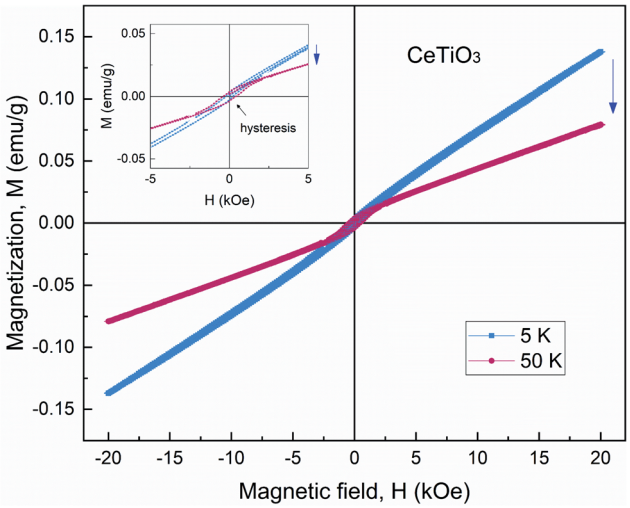

Fig. 4 Magnetization *vs.* applied magnetic field (*M*–*H*) curve of $CeTiO_3$ measured at 5 K and 50 K, respectively.

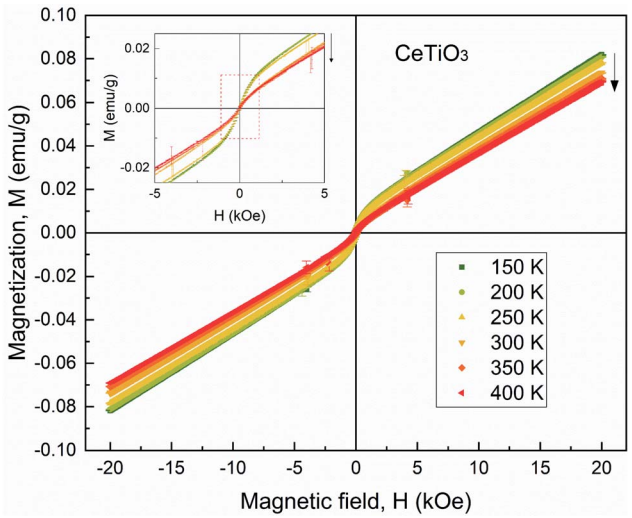

Fig. 6 Magnetization *vs.* applied magnetic field (*M*–*H*) curve of $CeTiO_3$ measured from 150 to 400 K.

Open Access Article. Published on 07 June 2022. Downloaded on 4/27/2026 4:14:30 AM.
This article is licensed under a Creative Commons Attribution-NonCommercial 3.0 Unported Licence.

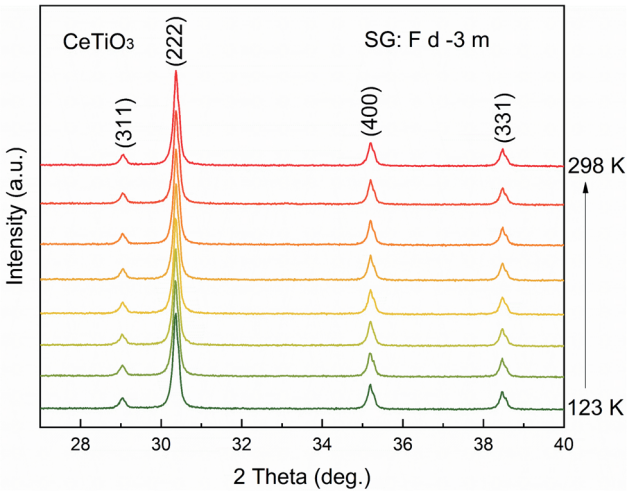

Fig. 7 Temperature dependence of XRD patterns from 123 to 298 K for the $CeTiO_3$.

a PANalytical diffractometer (Cu Kα, $\lambda = 1.5406$ Å) from −150 to 700 °C with the scanning rate of 4° min^{-1}. In order to stabilize the temperature, the warming rate was 5 °C min^{-1} and the waiting time is 5 min at each temperature. All the Rietveld refinements of the XRD data were performed on FULLPROF package.[21]

Results and discussions

As shown in Fig. 2, the *M–H* curves of $CeTiO_3$ measured at 300 K with different magnetic fields. It is clearly observed that weak ferromagnetic-like (FM-like) state occurs for $CeTiO_3$ at 300 K. However, the magnetization increases monotonously as the magnetic field increases up to 50 kOe. There is negligible change of magnetization such as metamagnetic transition in these three *M–H* curves, indicating the magnetic state of $CeTiO_3$ at 300 K might be a combination of FM and paramagnetic (PM) state and the FM state could be stronger upon cooling.[22,23]

Fig. 3 shows that the temperature dependence of magnetization curves were measured under applied magnetic field of 1000 Oe under zero field cooling and field cooling (ZFC–FC) from 5 to 350 K. The separation can be seen in ZFC–FC curves near 300 K and the *M–H* curves, indicating there is an obvious magnetic ordering transition from FM-like to PM near 300 K.[24,25] As the temperature decreases, the magnetization increases at first and then decreases subsequently. A maximum is observed near 150 K in *M–T* curves. No abrupt change emerges near this temperature range, which implies the maximum might be

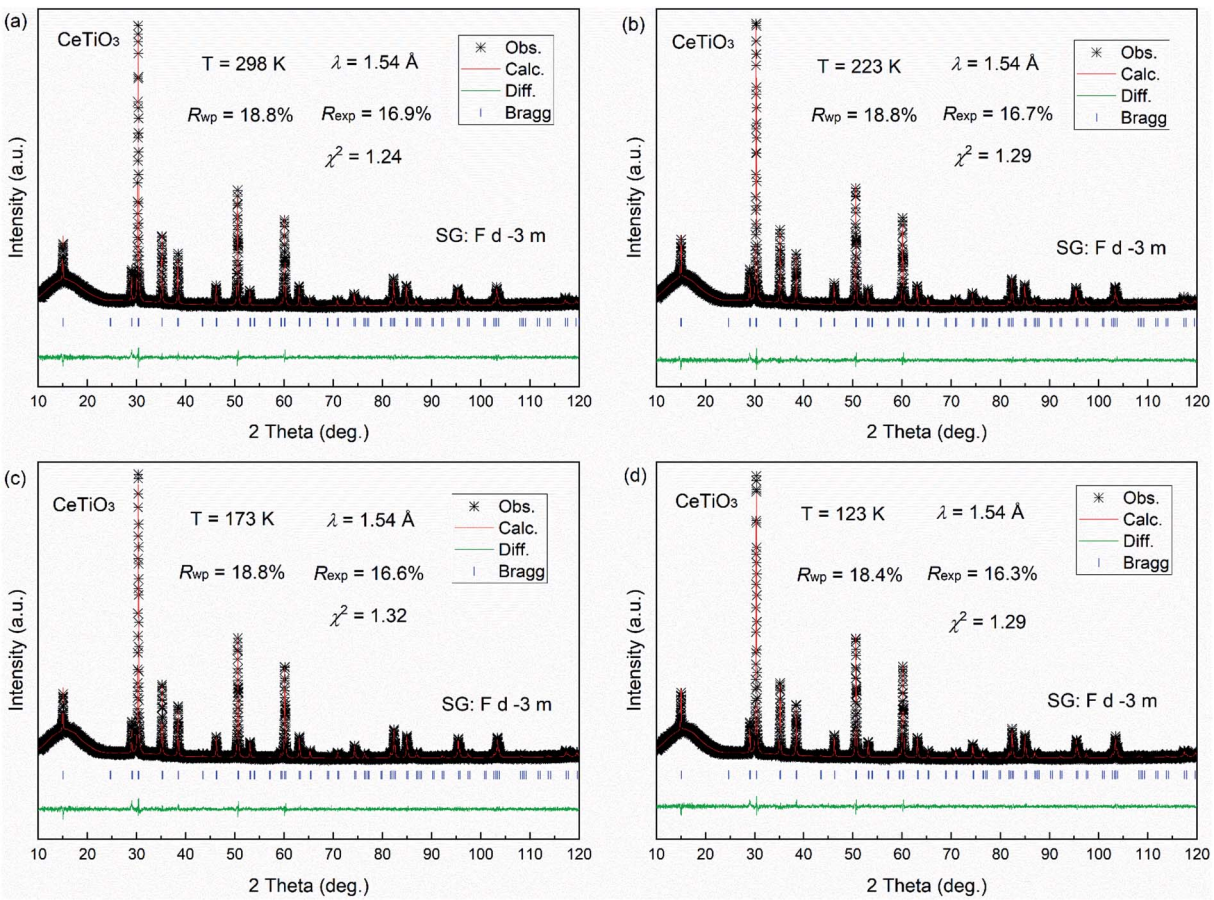

Fig. 8 (a) Rietveld refinements of XRD patterns at 123 K, (b) 173 K (c) 223 K and (d) 298 K, respectively.

© 2022 The Author(s). Published by the Royal Society of Chemistry

Open Access Article. Published on 07 June 2022. Downloaded on 4/27/2026 4:14:30 AM.
This article is licensed under a Creative Commons Attribution-NonCommercial 3.0 Unported Licence.

derived from the change of magnetic component. More interestingly below 150 K, the separation become more prominent between ZFC and FC, this means the magnetic ordering can be adjusted by magnetic field, which implies some antiferromagnetic (AFM) state might emerge below 150 K. Thereby, the total magnetization is thus weakened.[26] Intriguingly, an unusual magnetic behavior occurs below 32 K in ZFC and FC curves. The magnetization increases quickly in both ZFC and FC curves, demonstrating an intrinsic magnetic transition at 32 K. The increase of magnetization shows the positive exchange interaction may become stronger below 32 K, inconsistent with that above 32 K.[27]

To better understand the complicated magnetic evolution of the $CeTiO_3$, the isothermal magnetization *vs.* magnetic field (*M–H*) curves were measured from 5 to 400 K. As shown in Fig. 4, the *M–H* curves at 5 K and 50 K are plotted from −20 to 20 kOe, respectively. Notably, the configurations of the *M–H* at these two temperatures show little difference whereas the saturation magnetization changes remarkably. For example, the magnetization at 20 kOe is about 0.14 emu g^{-1} for 5 K and decreases near a half for 50 K (~0.08 emu g^{-1}), in good agreement with the *M–T* curves. To enlarge the region of *M–H* curves at low magnetic field from −5 to 5 kOe (the inset of Fig. 4), the distinct hysteresis and coercivity are observed in both 5 and 50 K. Interestingly, the coercivity of 5 K is smaller than that of 50 K, which indicates the magnetism is softened at 5 K. The FM-like state turns to dominate and the saturation magnetization increases accordingly. The apparent change of *M–H* curves can be attributed to the variable exchange interaction for the $CeTiO_3$.

The *M–H* curves at 50 K, 100 K and 150 K are shown in Fig. 5 from −20 to 20 kOe, respectively. Although the *M–H* curves are almost identical, the saturation magnetization increase a little from 50 to 150 K, consistent with the ZFC–FC curves. It should be noticed that the hysteresis and coercivity dramatically vanish at 100 K and 150 K, which demonstrate the magnetic component is sensitive to the temperature and hence contributes to the magnetization history. Upon heating, the saturation magnetization decreases and the FM-like state is weakened from 150 to 250 K (Fig. 6). The maximum is similar to that of *M–T* curves. A distinct change of *M–H* curves is determined between 250 K and 300 K, which indicates the magnetic

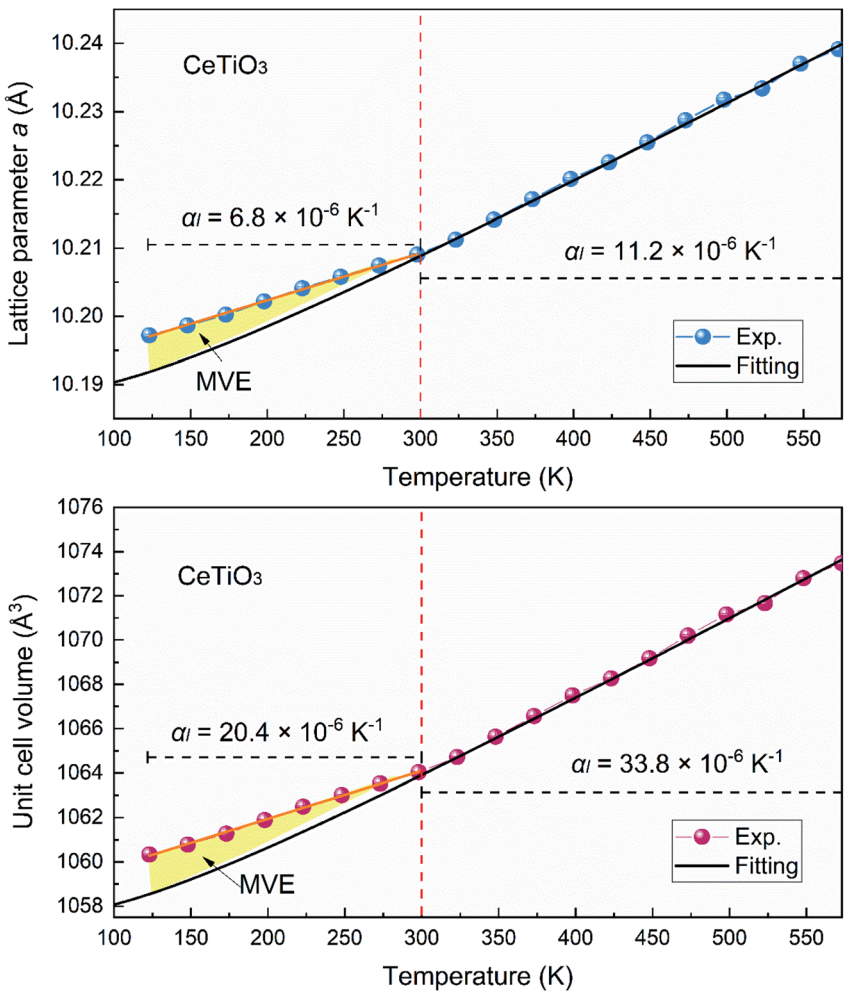

Fig. 9 Temperature dependence of lattice parameter *a* and unit cell volume *V* from 123 to 423 K for the $CeTiO_3$. The shadow indicates the magnetic contribution on the lattice.

Open Access Article. Published on 07 June 2022. Downloaded on 4/27/2026 4:14:30 AM. This article is licensed under a Creative Commons Attribution-NonCommercial 3.0 Unported Licence.

ordering becomes weak and the PM state emerges. Thereby, the magnetism above 300 K might be owing to the short-range ordering.[28,29]

The crystal structure at low temperature is studied by temperature dependence of XRD patterns from 123 to 423 K. for the $CeTiO_3$. As shown in Fig. 7, the XRD patterns are of good quality at each investigated temperature and no obvious change is observed for the peak reflections. Negligible change of peak shapes indicates that the cubic phase is stable at low temperature and there is no structural transformation upon cooling down to 123 K. All the XRD patterns were refined by the Rietveld refinement to determine the detailed structural information, as shown in Fig. 8. It clearly revealed that the crystal structure shows good cubic symmetry at each temperature. The peak intensities almost remain constant, which is well indexed into the symmetry of $Fd\bar{3}m$ with large vacancy of Ce ions.

Fig. 9 shows the temperature dependence of lattice parameter a and unit cell volume V from 123 to 423 K (Table 1). Although the lattice parameters increase monotonously with increasing temperature, there is an inflection near 300 K. Namely, positive thermal expansion (PTE) occurs over the entire investigated temperature window but the coefficient of thermal expansion (CTE) is different below 300 K. For example, average CTE along a direction is about 11.2×10^{-6} K^{-1} (300–423 K) and the CTEs of unit cell volume is 3 times as large as that of a axis, 33.8×10^{-6} K^{-1} (300–423 K). However, as temperature decreases, the CTE decreases below 300 K gradually. The average CTE along a direction is about 6.8×10^{-6} K^{-1} and that of unit cell volume is about 20.4×10^{-6} K^{-1}. A distinct decrease of CTE is determined below 300 K, which indicates another contribution on lattice might be emerge and compensate the nominal PTE derived from phonon effects.[30,31]

The comparison of Fig. 9 and 3 shows the thermal expansion anomaly exactly occurs over the magnetic ordering temperature window. This implies the magnetic ordering intimately entangles in the change of lattice thermal expansion below 300 K. This historically terms magnetovolume effect (MVE), which have been found in many magnetic materials since 1897.[32] To detect the MVE prominently, the nominal lattice thermal expansion is calculated by theoretically estimated by using the Debye equation that subtracts the magnetic contributions (Fig. 9).[33] It is noticed that the distinct MVE is observed below 300 K and increases gradually upon cooling. The MVE provides a positive contribution on lattice parameters. As the magnetic ordering is weakened, the MVE disappears and the abnormal expansion is observed subsequently for $CeTiO_3$. The further investigation on this spin–lattice coupling could be carried out by neutron powder diffraction in the future.

At 5 K, the saturation magnetization abruptly increases and the hysteresis decreases a little. This indicates the 5d electron of Ce ions might be less itinerant and the local moments of Ce ions increases, which benefits the FM ordering.[34] Upon heating, the itinerant electron is active and the magnetic exchange interaction become more flexible, generating magnetic competition. Thereby, the magnetic hysteresis is enhanced and saturation magnetization decreases. As the temperature approaches 300 K, thermal perturbation favors the suppression of magnetic ordering. Both magnetization and hysteresis will vanish for $CeTiO_3$. Such a complicated evolution of magnetic transition is rare in Ce–Ti–O perovskite oxides.

Table 1 Lattice parameters of $CeTiO_3$ from 123 K to 423 K

Temperature (K)	Lattice parameter a (Å)	Unit cell volume V (Å^3)
123	10.19719(19)	1060.331(34)
148	10.19864(20)	1060.782(35)
173	10.20022(20)	1061.275(36)
198	10.20217(20)	1061.884(36)
223	10.20411(20)	1062.491(37)
248	10.20578(20)	1063.011(36)
273	10.20744(21)	1063.531(38)
298	10.20905(16)	1064.036(29)
323	10.21123(16)	1064.717(29)
348	10.21416(18)	1065.635(32)
373	10.21715(18)	1066.569(33)
398	10.22012(20)	1067.500(36)
423	10.22256(21)	1068.266(38)

Conclusion

To conclude, the magnetic behaviors and lattice thermal expansion at low temperature were systematically investigated by temperature dependence of magnetization measurements and low temperature X-ray powder diffraction. It is clearly revealed that there is two magnetic transition in the cubic $CeTiO_3$ from 5 to 350 K: one is magnetic ordering–disordering transition at 300 K and the other one might be the change of magnetic component near 32 K. The magnetization and hysteresis can change correspondingly upon cooling. Intriguingly, lattice thermal expansion anomaly is found below magnetic ordering temperature, which indicates a strong coupling of spin and lattice, *i.e.*, magnetovolume effect (MVE). This work gives a good understanding of the unusual magnetic behaviors of $LnBO_3$-based perovskite oxides.

Conflicts of interest

There are no conflicts to declare.

Acknowledgements

This study was financially supported by Fundamental Research Funds for the Central Universities of China (No. FRF-BR-20-03B) and National Key R&D Program of China No. 2017YFF0106006.

Notes and references

1 H. Zhu, P. Zhang and S. Dai, *ACS Catal.*, 2015, **5**, 6370–6385.
2 J. Y. Han and C. W. Bark, *J. Korean Phys. Soc.*, 2015, **66**, 1371–1375.
3 H. Chen, W. Cui, D. Li, Q. Tian, J. He, Q. Liu, X. Chen, M. Cui, X. Qiao and Z. Zhang, *Ind. Eng. Chem. Res.*, 2020, **59**, 10804–10812.

© 2022 The Author(s). Published by the Royal Society of Chemistry

Open Access Article. Published on 07 June 2022. Downloaded on 4/27/2026 4:14:30 AM.
This article is licensed under a Creative Commons Attribution-NonCommercial 3.0 Unported Licence.

4 R. Roukos, N. Zaiter and D. Chaumont, *J. Adv. Ceram.*, 2018, **7**, 124–142.
5 I. N. Sora, T. Caronna, F. Fontana, C. de Julián Fernández, A. Caneschi and M. Green, *J. Solid State Chem.*, 2012, **191**, 33–39.
6 C. Si, C. Zhang, J. Sunarso and Z. Zhang, *J. Mater. Chem. A*, 2018, **6**, 19979–19988.
7 S. Stramare, V. Thangadurai and W. Weppner, *Chem. Mater.*, 2003, **15**, 3974–3990.
8 J. Ma, Y. Zhai, R. Xu, H. Zhang and Q. Chen, *Ceram. Int.*, 2021, **47**, 19659–19667.
9 J.-M. Li, C. Huan, Y.-W. Du, D. Feng and Z.-X. Shen, *Phys. Rev. B: Condens. Matter Mater. Phys.*, 2000, **63**, 024416.
10 X. Li, D. Chen, N. Li, Q. Xu, H. Li, J. He and J. Lu, *J. Alloys Compd.*, 2021, **871**, 159575.
11 B. Nagabhushana, G. Chandrappa, R. S. Chakradhar, K. Ramesh and C. Shivakumara, *Solid State Commun.*, 2005, **136**, 427–432.
12 H. Hwang, S. Cheong, P. Radaelli, M. Marezio and B. Batlogg, *Phys. Rev. Lett.*, 1995, **75**, 914.
13 C. Ritter, M. Ibarra, J. De Teresa, P. Algarabel, C. Marquina, J. Blasco, J. Garcia, S. Oseroff and S. Cheong, *Phys. Rev. B: Condens. Matter Mater. Phys.*, 1997, **56**, 8902.
14 M. Pena and J. Fierro, *Chem. Rev.*, 2001, **101**, 1981–2018.
15 J.-M. Li, X.-L. Zeng and Z.-A. Xu, *Appl. Phys. Lett.*, 2013, **103**, 232410.
16 J.-D. Li, A.-J. Gong, X.-Y. Li, Y.-F. He, J.-S. Li, Y.-Z. Bai and R.-R. Fan, *RSC Adv.*, 2022, DOI: **10.1039/d2ra01714h**.
17 K. Yoshii and H. Abe, *J. Alloys Compd.*, 2002, **343**, 199–203.
18 J. Goral and J. Greedan, *J. Magn. Magn. Mater.*, 1983, **37**, 315–321.
19 A. G. Bhavani, W. Y. Kim and J. S. Lee, *ACS Catal.*, 2013, **3**, 1537–1544.
20 Y.-H. Huang, Z.-G. Xu, C.-H. Yan, Z.-M. Wang, T. Zhu, C.-S. Liao, S. Gao and G.-X. Xu, *Solid State Commun.*, 2000, **114**, 43–47.
21 J. Rodríguez-Carvajal, *CEA/Saclay*, France, 2001.
22 T. Kaneyoshi, *J. Magn. Magn. Mater.*, 1995, **140**, 261–262.
23 T. Jacobs, K. Buschow, G. Zhou, X. Li and F. De Boer, *J. Magn. Magn. Mater.*, 1992, **116**, 220–230.
24 M. F. Hansen and S. Mørup, *J. Magn. Magn. Mater.*, 1999, **203**, 214–216.
25 M. Jeddi, H. Gharsallah, M. Bekri, E. Dhahri and E. Hlil, *Appl. Phys. A*, 2020, **126**, 1–10.
26 E. Chi, W. Kim and N. Hur, *Solid State Commun.*, 2001, **120**, 307–310.
27 P. Tong, B.-S. Wang and Y.-P. Sun, *Chin. Phys. B*, 2013, **22**, 067501.
28 R. Nag, B. Sarkar and S. Pal, *J. Magn. Magn. Mater.*, 2018, **449**, 21–24.
29 T. Phan, P. Tola, N. Dang, J. Rhyee, W. Shon and T. Ho, *J. Magn. Magn. Mater.*, 2017, **441**, 290–295.
30 T. Hamada and K. Takenaka, *J. Appl. Phys.*, 2011, **109**, 07E309.
31 K. Takenaka and H. Takagi, *Appl. Phys. Lett.*, 2005, **87**, 261902.
32 J. Chen, L. Hu, J. Deng and X. Xing, *Chem. Soc. Rev.*, 2015, **44**, 3522–3567.
33 P. Miao, X. Lin, A. Koda, S. Lee, Y. Ishikawa, S. Torii, M. Yonemura, T. Mochiku, H. Sagayama, S. Itoh, K. Ikeda, T. Otomo, Y. Wang, R. Kadono and T. Kamiyama, *Adv. Mater.*, 2017, **29**, 1605991.
34 K. Takenaka, *Front. Chem.*, 2018, **6**, 267.

© 2022 The Author(s). Published by the Royal Society of Chemistry